

MODELLING AND SIMULATION OF THE MECHANICAL BEHAVIOUR OF WEFT-KNITTED FABRICS FOR TECHNICAL APPLICATIONS

Part II: 3D model based on the elastica theory

M. de Araújo, R. Figueiro and H. Hong¹

University of Minho, Guimarães, Portugal

Phone: +351 253 510 280 Fax: +351 253 510293

maraujo@det.uminho.pt; rfang@det.uminho.pt

Abstract

This paper is in four parts. The first is related to general considerations and experimental analyses, and each of the others is related to different approaches to the theoretical analyses of the mechanical behaviour of weft-knitted fabrics and weft-knitted reinforced composites made of glass fibre. The objective is to find ways of improving the mechanical properties and simulating the mechanical behaviour of knitted fabrics and knitted reinforced composites so that the engineering design of such materials and structures may be improved.

In Part II the first model is presented, a 3D model based on the classic elastica theory which is used to calculate the load-extension curves of a plain weft-knitted fabric in the coursewise and walewise directions. Good agreement is obtained between theoretical and experimental results.

Keywords:

Knitted fabric, load-extension curve, technical textiles, modelling, mechanical properties, composite materials

1. INTRODUCTION

Various investigations into the tensile properties of plain weft-knitted fabrics have been carried out by various authors [1, 2, 3, 4, 5, 6, 7, 8, 9]. Most of these investigations were based on the micro-mechanics of knitted structures. The unit cell, often a single loop, was used for the analyses. The tensile properties of knitted fabrics were directly derived from the loop configuration and the yarn properties. However, these analyses were mostly limited to knitted fabrics subjected to biaxial stresses. The model proposed by Shanahan and Postle [8] related to the analyses of knitted fabrics under uniaxial stress conditions in the coursewise direction. It should be stressed that most of these models are difficult to apply in practice, due to their complexity.

In this paper, a theoretical analysis based on the elastica theory is proposed for the prediction of both uniaxial and biaxial tensile properties of plain knitted fabrics made from high performance fibres. In order to validate the model, the theoretical results are compared with experimental data for fabrics subjected to extensions in both walewise and coursewise directions [10].

2. ANALYSIS

2.1. Basic assumptions

(1) The plain knitted fabrics are made of frictionless, inextensible, incompressible and naturally straight filament yarns, which can be considered as a homogeneous elastic rod. This assumption is not very realistic, but should be accepted for two reasons. Firstly, our analysis is focused on the deformation of knitted fabrics at low loading conditions (compared to the load required to break the yarn). In this condition, the chief mechanism of deformation is the change of the loop shape within the fabric. The resistance to extension of the fabric depends mainly on the bending and torsional properties of the yarn. In this case, yarn friction, extension and compression effects are relatively small and can be

¹ Currently at Dong Hua Textile University, Shanghai, China

ignored. The second reason is that the knitted fabric to be analysed is made from high performance yarns. These are less compressible and extensible than the yarns conventionally used for clothing.

(2) The knitted fabric is formed with planar loop structures. All loops within the same fabric keep an identical configuration. No plastic deformation of the yarn takes place when the fabric is knitted from a straight yarn and later subjected to extension. The load-extension properties of a knitted fabric are directly derived from its loop configuration change.

(3) Two loops at adjacent courses interlock in such a way that the yarns of the two loops are fully in contact at the cross-regions. The distance between the interlocking points B-B' of two neighbouring loops, as shown in Figure 1, is equal to the diameter of the yarn.

(4) The reaction forces produced in the loop-interlacing region due to yarn contact are simplified as a concentrated force. As shown in Figure 1, the reaction forces R act at the loop-interlocking points B and B' and along a line perpendicular to the yarn axis. This assumption is similar to the two-dimensional model proposed for dry-relaxed knitted fabrics by Postle & Munden [11] and that for the analysis of the tensile properties parallel to the course direction by Shanahan & Postle [1]. However, in the present model, the point of application and the direction of the forces R are not assumed to be constant or parallel to the course direction; they are assumed to change with the state of the loop extension. The advantage of this assumption is that the yarn slippage effects are automatically included in the analysis.

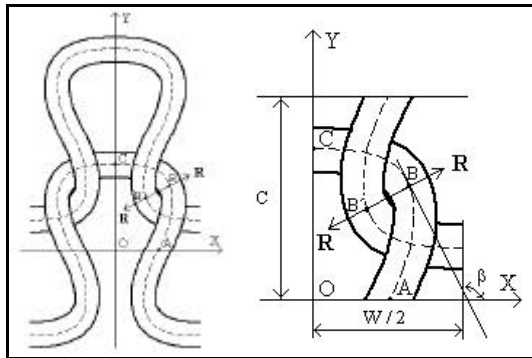


Figure 1. Loop structure and repeating elements

2.2. Theoretical Analysis

Due to the symmetry of the loop configuration, only a quarter of the loop is analysed.

2.2.1. Geometrical relations

The global reference system XOY is set up as shown in Figure 1. By considering the geometrical configuration of the loop, the following equations are obtained:

$$W / 4 = X_B - (d / 2) \cos(\beta - \pi / 2) \quad (1)$$

$$C / 2 = Y_B - (d / 2) \sin(\beta - \pi / 2) \quad (2)$$

$$X_B - X_A = (d / 2) \cos(\beta - \pi / 2) \quad (3)$$

$$L / 4 = s_{AB} + s_{BC} \quad (4)$$

where:

W - wale-spacing,

C - course-spacing,

X_A , X_B and Y_B - coordinates of points A and B in XOY,

d - diameter of the yarn,

β - the angle which the tangent of yarn axis at B forms with the positive direction of the X-axis,

L - loop length,

s_{AB} and s_{BC} - lengths of segments AB and BC.

2.2.2. Force-equilibrium consideration

As shown in Figure 2, the quarter-loop is divided into two segments, AB and BC, by the force R. By considering the symmetrical properties of the loop and the force-equilibrium state, the forces and

moment applied at points A and C can be derived. At point A, only force P is applied. No moment is applied at this point because it is an inflexion point. It should be pointed out that the force P is not parallel to the tangent of the axis at A; its direction relative to the X-axis changes with the loop configuration. The force P can be divided into two components, P_x and P_y , where P_y corresponds to the stress applied in the walewise direction. At point C, besides force T, acting parallel to the X-axis, there is a bending moment M. The force T corresponds to the stress in the coursewise direction.

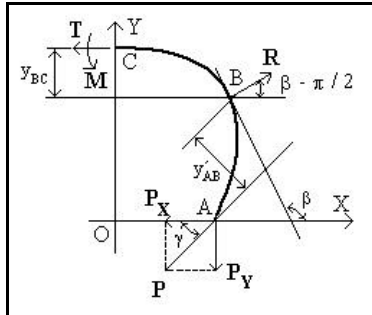


Figure 2. Forces and moment applied on a quarter of loop

Based on the force-equilibrium state, the relationships between T, P and M can be obtained:

$$T = -P (\sin\gamma \tan\beta + \cos\gamma) \quad (5)$$

$$M = P \{y'_{AB} + y_{BC} (\sin\gamma \tan\beta + \cos\gamma)\} \quad (6)$$

where:

- γ - the angle the force P forms with the negative direction of the X – axis,
- y'_{AB} - the perpendicular distance from point B to the line of action of P,
- y_{BC} - the perpendicular distance from point B to the line of action of T.

2.2.3. Analysis based on the elastica theory

(1) Analysis of segment AB

The analysis of this segment is identical to the analysis of an elastica with a single force applied at its extremity. As shown in Figure 3, to simplify the analysis, the reference system XOY was transformed to $x'A'y'$ where the x' -axis coincides with the line of action of the force P.

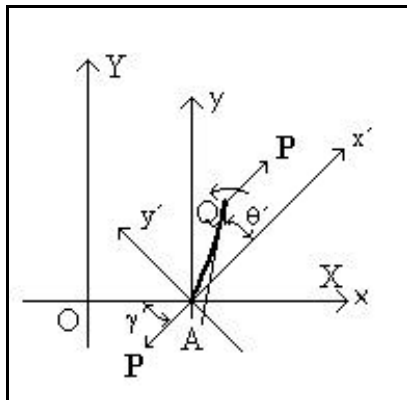


Figure 3. Analysis of the segment AB

By considering any point Q(x' , y') on segment AB and taking bending moments about A, the following differential equation is obtained:

$$B d\theta' / ds' = P y' \quad (7)$$

where B is the bending rigidity of the yarn.

The integration of equation 7 from A to B gives the following results:

$$x'_{AB} = (B/P)^{1/2} \{f(\epsilon_1, \phi_{1B}) - 2e(\epsilon_1, \phi_{1B})\} \quad (8)$$

$$y'_{AB} = 2(B/P)^{1/2} \epsilon_1 \cos\phi_{1B} \quad (9)$$

$$s_{AB} = (B/P)^{1/2} f(\epsilon_1, \phi_{1B}) \quad (10)$$

where:

α - the angle the tangent to the loop at A forms with the positive direction of the X-axis,
 $\varepsilon_1 = \cos((\alpha - \gamma) / 2)$,
 $\varphi_{1B} = \arcsin(\cos((\beta - \gamma) / 2) / \varepsilon_1)$,
 x'_{AB}, y'_{AB} - the coordinates of the point B in the new reference system $x'Ay'$,
 $f(\varepsilon_1, \varphi_{1B}) = F(\varepsilon_1, \pi / 2) - F(\varepsilon_1, \varphi_{1B})$,
 $e(\varepsilon_1, \varphi_{1B}) = E(\varepsilon_1, \pi / 2) - E(\varepsilon_1, \varphi_{1B})$.

$F(\varepsilon_1, \pi / 2)$ and $F(\varepsilon_1, \varphi_{1B})$ are respectively complete and incomplete elliptical integrals of the first kind.
 $E(\varepsilon_1, \pi / 2)$ and $E(\varepsilon_1, \varphi_{1B})$ are respectively those of the second kind.
The coordinate transformation gives the following equations:

$$X_B - X_A = x'_{AB} \cos\gamma - y'_{AB} \sin\gamma \quad (11)$$

$$Y_B = x'_{AB} \sin\gamma + y'_{AB} \cos\gamma \quad (12)$$

(2) Analysis of segment BC

The analysis of this segment is very similar to that of segment AB. The difference is that, besides the force T, there is still a bending moment M acting at its extremity.

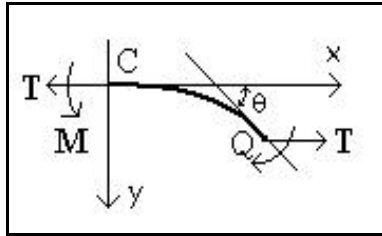


Figure 4. Analysis of segment BC

The reference system xCy used for the analysis in this case is shown in Figure 4. By considering any point $Q(x, y)$ and taking moments about C, the following differential equation is obtained:

$$B \, d\theta / ds = T y + M \quad (13)$$

The integration of equation 13 from C to B and the elimination of T and M through equations 5, 6 and 8 lead to the following results:

$$X_B = (B / P)^{1/2} (1 / k_2)^{1/2} [(2 / \varepsilon_2^2) E(\varepsilon_2, \varphi_{2B}) + \{1 - (2 / \varepsilon_2^2)\} F(\varepsilon_2, \varphi_{2B})] \quad (14)$$

$$s_{BC} = (B / P)^{1/2} (1 / k_2)^{1/2} F(\varepsilon_2, \varphi_{2B}) \quad (15)$$

where:

$$k_2 = 2 \varepsilon_1^2 \cos^2 \varphi_{1B} + k_1 \cos\beta, k_1 = \sin\gamma \tan\beta + \cos\beta,$$

$$\varepsilon_2 = \{k_1 / (k_2 + k_1)\}^{1/2},$$

$$\varphi_{2B} = (\beta - \pi) / 2.$$

$F(\varepsilon_2, \varphi_{2B})$ and $E(\varepsilon_2, \varphi_{2B})$ are elliptical integrals of the first and second kinds respectively.

2.2.4. General equations for the description of any loop state

By substituting $X_B, Y_B, X_B - X_A, s_{AB}$ and s_{BC} into equations 1 to 4 from equations 14, 12, 11, 10 and 15, and by eliminating P, the following general equations for the description of any loop configuration are obtained:

$$L / W = C_4 / (C_1 - C_3) \quad (16)$$

$$L / C = C_4 / (C_2 + \cot\beta C_3) \quad (17)$$

$$L / d = 2 \sin\beta C_4 / C_3 \quad (18)$$

where:

$$C_1 = (1 / k_2)^{1/2} [(2 / \varepsilon_2^2) E(\varepsilon_2, \varphi_{2B}) + \{1 - (2 / \varepsilon_2^2)\} F(\varepsilon_2, \varphi_{2B})]$$

$$C_2 = \sin\gamma \{ f(\varepsilon_1, \varphi_{1B}) - 2 e(\varepsilon_1, \varphi_{1B}) \} + 2 \cos\gamma \varepsilon_1 \cos\varphi_{1B}$$

$$C_3 = \cos\gamma \{f(\varepsilon_1, \varphi_{1B}) - 2 e(\varepsilon_1, \varphi_{1B})\} - 2 \cos\gamma \varepsilon_1 \sin\varphi_{1B}$$

$$C_4 = f(\varepsilon_1, \varphi_{1B}) + (1/k_2)^{1/2} F(\varepsilon_2, \varphi_{2B})$$

C_1, C_2, C_3 and C_4 are functions of the angles α, β and γ .

The equations 16 to 18 are non-linear equations, which have no analytical solution. Thus, numerical methods are necessary to solve them. When L, W, C and d are given, α, β, γ at any deformed state can be evaluated numerically. When α, β, γ and B are known, P can be calculated from the following equation:

$$P = 16 C_4^2 L^2 \quad (19)$$

and T from equation 5.

3. THEORETICAL CALCULATION AND COMPARISON WITH EXPERIMENTAL RESULTS

3.1. Parameters used for calculations and tensile testing

The parameters measured on a knitted fabric produced from glass fibre filament yarn prior to testing are shown in Table 1. These were used for the theoretical calculation of the tensile properties.

Table 1. Parameters used for the calculations

L [mm]	C [mm]	W [mm]	d [mm]	B [N mm ²]
7.46	1.58	1.88	0.461	0.11

Tensile testing was performed on a Hounsfield HI0KS universal tester according to ASTM D 2256-88. Due to the high rigidity of the glass fibre yarn, it was not possible to cut the fabric to the specified sample dimensions (the fabric unravels automatically after cutting). For this reason, the samples of the required dimensions were directly knitted to size on an electronic flat knitting machine (10 for coursewise testing and 10 for walewise testing). The experimental load-extension curves used for the comparison (see Figures 5 and 6), are the average values of 10 test results in each direction. The statistical coefficient of variation (CV%) was 5.6% in the walewise direction and 7.3% in the coursewise direction.

3.2. Initial state

The initial state is the reference state, which is also a zero-loading state. The results of the calculation for the initial state are given in Table 2.

Table 2. Results of the calculation for the initial state

α_0	β_0	γ_0	T_0 [N]	P_0 [N]
63.0°	98.4°	9.0°	0.013	0.165
P_{x0} [N]	P_{y0} [N]	M_0 [N mm]	s_{AB0} [mm]	s_{BC0} [mm]
0.163	0.026	0.121	0.869	0.996

These results show that T_0 and P_{y0} do not equal zero. This means that the initial state of the knitted fabric used for the calculation is not a completely relaxed state. For this reason, the load applied in the wale direction must be equal to $P_y - P_{y0}$ and that applied in the course direction must be equal to $T - T_0$, where T, P_y and T_0, P_{y0} are the forces applied to the loop at the extended state and at the initial state respectively.

3.3. Extension in the walewise direction

When a knitted fabric is extended along its walewise direction, the width in the coursewise direction will be reduced. However, this reduction is limited by jamming of the loop structure in the coursewise

direction. For this reason, the conditions used for the calculation must be different before jamming and after jamming.

Before the occurrence of jamming in the width direction, equation 17 cannot be used for the calculation, because the value of the course spacing C needed to extend the fabric until jamming occurs is unknown. In order to calculate α , β and γ , the condition $T = T_0$ is assumed during the extension from the initial state until jamming occurs. By using this condition and equations 16 and 18, we can calculate α , β and γ for any given loop configuration up to jamming. At the jamming condition in the course direction, the wale spacing W is equal to four yarn diameters. As the yarn has been assumed to be incompressible, W remains constant after jamming. By using the condition $W = 4 d$ and equations 17 and 18, α , β and γ for any loop configuration after jamming occurs can be calculated. When the loop parameters α , β and γ are known, the forces applied to the loop can be determined. From this, the load-extension curves can be calculated.

Figure 5 shows the load-extension curves calculated and obtained from the experiments respectively. Observing these curves, it can be seen that the calculated curve is very close to the experimental one.

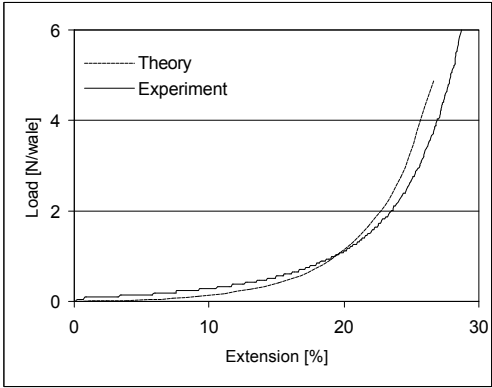


Figure 5. Extension in the walewise direction

3.4. Extension in the coursewise direction

When a knitted fabric is extended along its coursewise direction, the length in the walewise direction will also be reduced. For a given extension in the course direction, the value of the reduction in the walewise direction is not determined. In this case, equation 17 cannot be used for the calculation, because C has not been defined. In fact, when the extension is parallel to the coursewise direction, the segment BC of the loop will be stretched. For this reason, s_{BC} is assumed to be constant. By using this condition and equations 16 and 18, we can calculate α , β and γ for any given loop configuration in extension in the course direction.

Figure 6 shows the calculated load-extension curve and the one obtained from the experimental results. As the present model is similar to the one given by Shanahan & Postle for the extension in the coursewise direction, their results are also shown in Figure 6. Their curve, calculated up to 30% extension, was derived from Figure 5 on paper [1] for the condition at constant yarn diameter. Observing these results, it can be seen that the curves calculated from the two models, are very close.

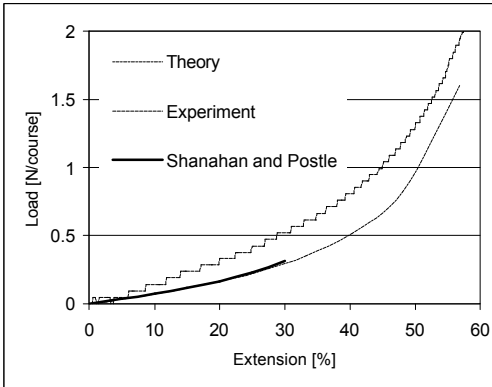


Figure 6. Extension in the coursewise direction

This means that the differences caused by changing the direction of the contact force R with the state of the loop extension are not significant in the coursewise direction. However, the assumption of changing the direction of R in the present model enabled us to use this unique model for the calculation of the tensile properties of the knitted fabrics both in the coursewise and walewise directions. The calculations of the biaxial tensile properties are also possible with the present model. It can also be seen from Figure 6 that even though the calculated results from the two models were lower than those obtained experimentally, they are quite close to each other.

4. CONCLUSION

A theoretical model, based on elastica theory and used for the prediction of the tensile properties of plain knitted fabrics produced from high performance yarns such as glass fibre, has been presented. Both walewise and coursewise directions of extension were considered. The load-extension curves parallel to the walewise and coursewise directions for a given knitted fabric were calculated theoretically and compared with the experimental results. Good agreement was found between theoretical and experimental values. This approach may lead to a reduction in the need for destructive testing, especially in the case of knitted fabrics produced with high modulus yarns such as glass fibre, and will thus be a more effective use of resources. Apart from the prediction of uniaxial tensile properties, the present model may also be used to calculate the biaxial tensile properties of plain knitted fabrics.

References

1. Hepworth, B. (1978), *J. Text. Inst.*, **4**, 101.
2. Kawabata, S., Niwa, M., Nanashima, Y., and Kawai, K. (1970), *J. Text. Mach. Soc. Japan*, **23**, T120.
3. Kawabata, S., Niwa, M., Nanashima, Y., and Kawai, K. (1970), *J. Text. Mach. Soc. Japan*, **23**, T223.
4. MacRory, B. M., McCraith, J. R., and McNamara, A. B. (1975), *Text. Res. J.*, **45**, 746.
5. MacRory, B. M., and McNamara, A. B. (1967), *Text. Res. J.*, **37**, 908.
6. Niwa, M., Kawabata, S., Nanashima, Y., and Kawai, K. (1970), *J. Text. Mach. Soc. Japan*, **23**, T120.
7. Popper, P. (1966), *Text. Res. J.*, **36**, 148.
8. Shanahan, W. J., and Postle, R. (1974), *Text. Res. J.*, **65**, 200.
9. Wu, W. L., Hamada, H., and Maekava, Z. I. (1994), *J Text. Inst.*, **85**, 199.
10. Hong, H, de Araújo, M. D. and Fanguero, R.(2002), *Textile Research Journal*, Vol.72, p.991-995, November.
11. Chou, T.W., and Ko, Frank K. (1989), *Textile Structural Composites*, Elsevier Science Publishing Company, Inc.